

## Supporting Information

### **Preparation of Cellulose Nanocrystal Reinforced Poly(lactic acid) Nanocomposites Through Non-covalent Modification with PLLA-based Surfactants**

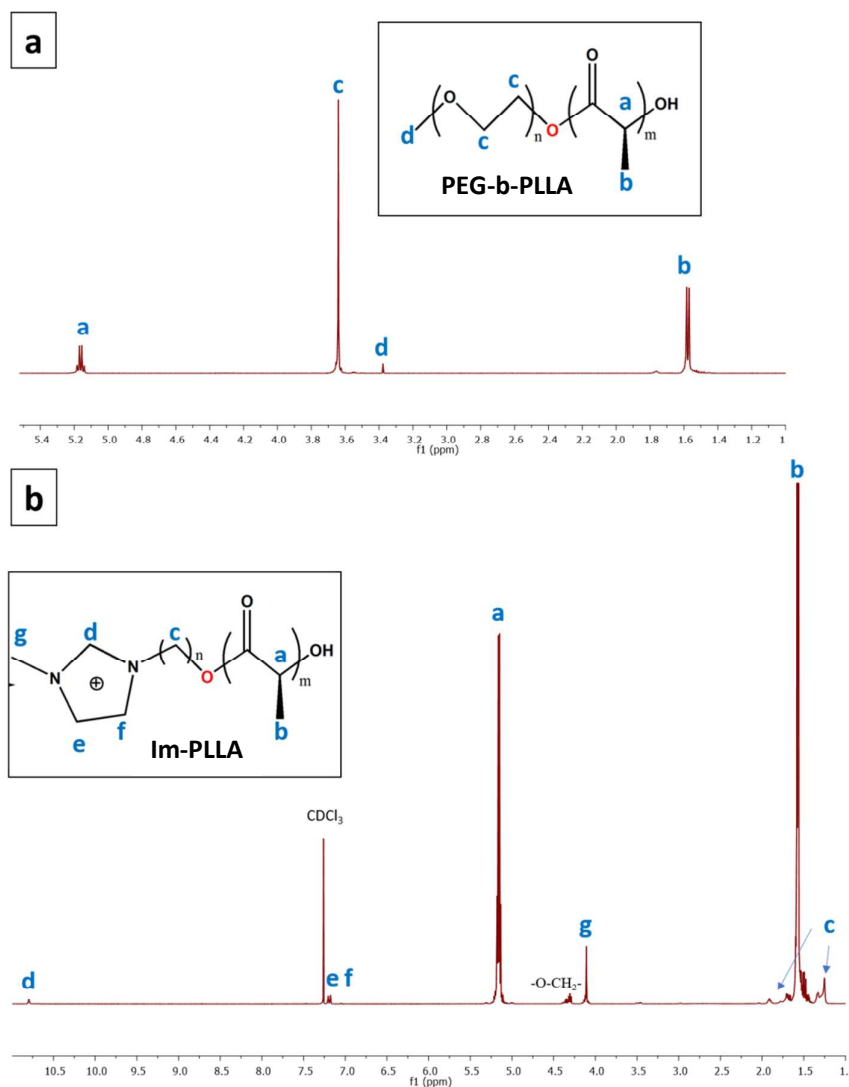
*Marcos Mariano,<sup>†</sup> Florence Pilate,<sup>§</sup> Franciéli Borges de Oliveira,<sup>†</sup> Farid Khelifa,<sup>§</sup> Philippe Dubois,<sup>§,⊥</sup> Jean-Marie Raquez,<sup>§</sup> Alain Dufresne<sup>\*†</sup>*

<sup>†</sup> Univ. Grenoble Alpes, CNRS, Grenoble INP\*\*, LGP2, F-38000 Grenoble, France

<sup>§</sup> LPCM, CIRMAP, University of Mons (UMONS), Place du Parc 20, B-7000 Mons, Belgium

<sup>⊥</sup> Department Materials Research and Technology, Luxembourg Institute of Science and Technology (LIST), Z.A.E. Robert Steichen, 5 Rue Bommel, L-4940 Hautcharage, Luxembourg

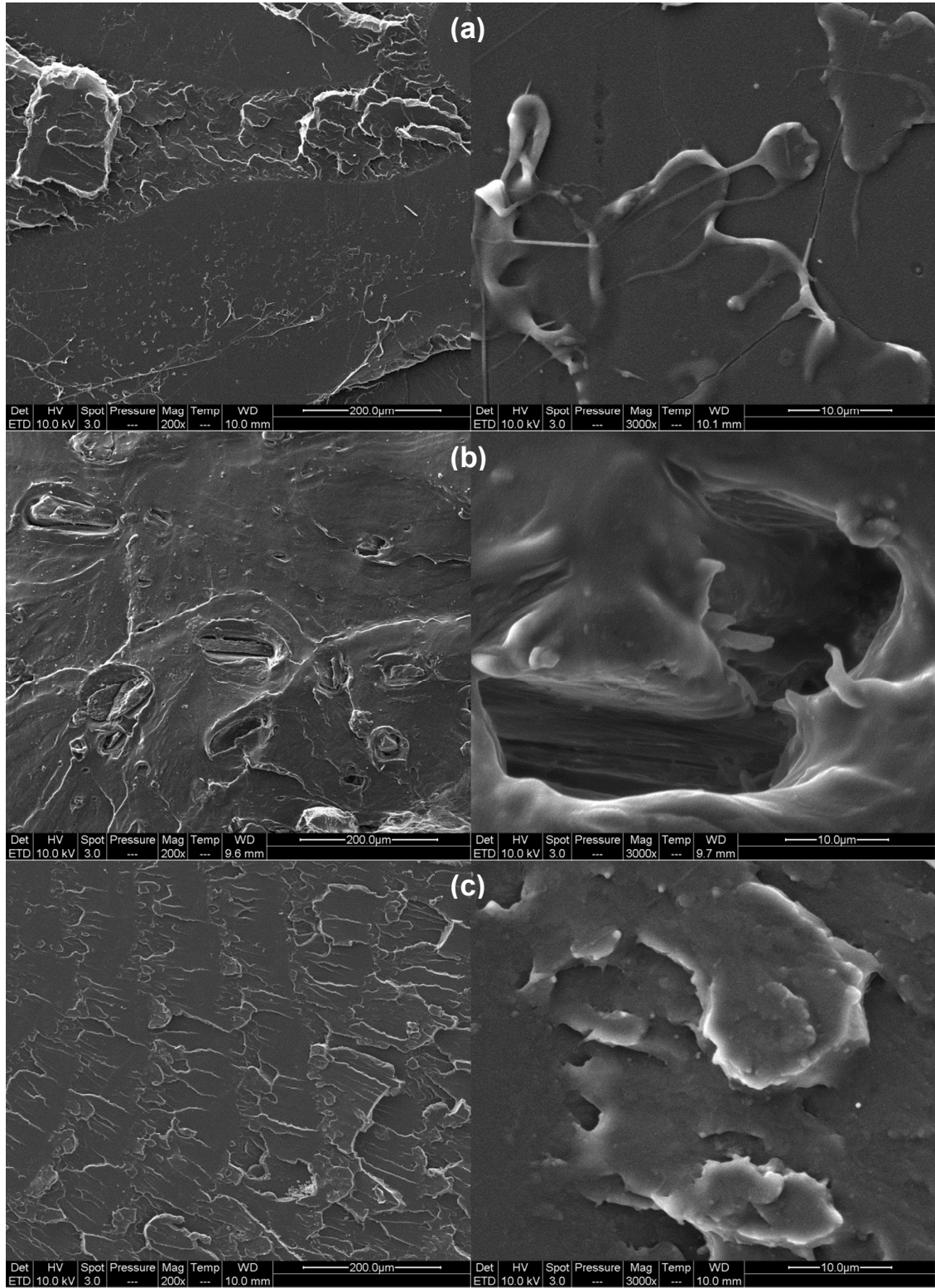
**Preparation of PLA-based surfactants.** PEG-b-PLLA was synthesized from L-lactide (17.58 g; 121.5 mmol) and poly(ethylene glycol) monomethyl ether (8.61 g; 4.3 mmol). Im-PLLA was prepared from L-Lactide (17.60 g; 121.5mmol) and from 1-(11-hydroxy-undecyl)-3-methylimidazolium bromide (1.43g; 4.3mmol) which was prepared by refluxing reaction between 1-methylimidazole and 11-bromoundecanol in chloroform as previously reported in the literature.<sup>1</sup>The *L*-Lactide and the initiator (PEG or Im) were first dissolved in chloroform (~ 65 mL) under magnetic stirring. Then, 132  $\mu$ L (1.075 mmol) of DBU was added and the reactions were conducted for 5 min in the case of Im-PLA and 10 min in the case of PEG-g-PLLA at ambient temperature. Then, 3 drops of glacial acetic acid were added to the resulting mixture and PEG-b-PLLA or Im-PLLA was collected by precipitation in heptane and filtration. The white powders were dried at 90°C under vacuum overnight. The yield was nearly complete for PEO-b-PLLA and Im-PLLA.



**Figure S1.**  $^1\text{H}$ -NMR spectra for (a) PEG-b-PLLA and (b) Im-PLLA surfactants.

PEG-b-PLLA:  $M_{n(\text{PS})}$  determined by SEC= 10,000  $\text{g/mol}^{-1}$ ,  $\bar{D}$ =1.77,  $^1\text{H}$  NMR ( $\text{CDCl}_3$ ):  $\delta$  5.16 (q,  $\text{CH-CH}_3$ ), 3.64 (t,  $\text{CH}_2$  (PEO block)), 3.37 (s,  $\text{CH}_3$  chain-end PEO), 1.58 (d,  $\text{CH}_3$  PLLA block).

Im-PLLA:  $M_{n(\text{PS})}$  determined by SEC= 1,300  $\text{g/mol}^{-1}$ ,  $\bar{D}$ =3.7,  $^1\text{H}$  NMR ( $\text{CDCl}_3$ ):  $\delta$  10.80 (s, CH), 7.20 & 7.18 (d,  $\text{CH}=\text{CH}$ ), 5.16 (q, CH), 4.31 (t,  $\text{O-CH}_2$ ) 1.62 (m,  $\text{CH}_2$ ), 1.58 (d,  $\text{CH}_3$ ), 1.3 (m,  $\text{CH}_2$ ).



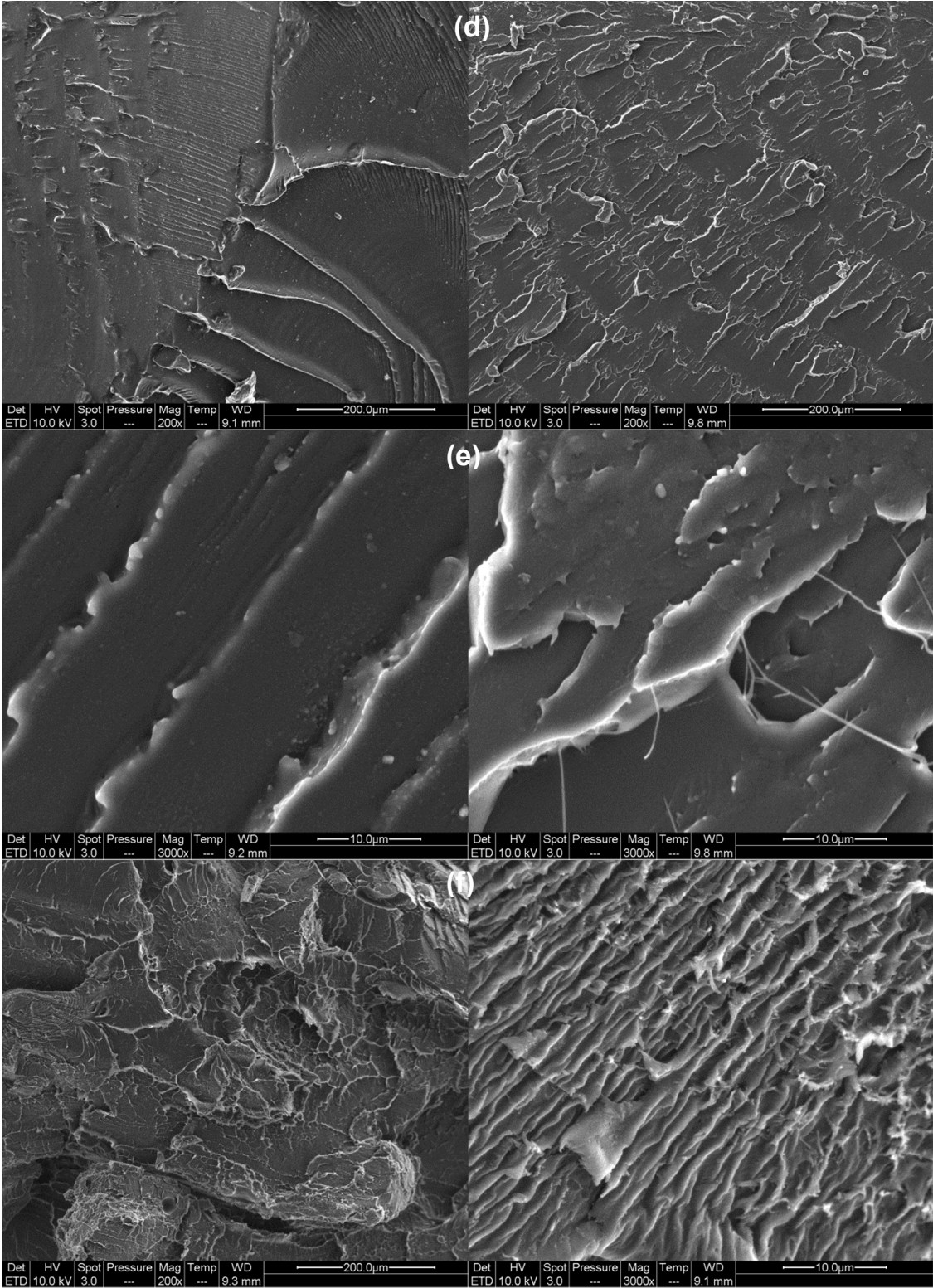


**Figure S2.** Typical SEM images of the tensile fracture cross-section for (a) PLA, (b) PLA<sub>5CNC</sub>, (c) PLA<sub>Im-PLLA</sub>, (d) PLA<sub>Im-PLLA+10CNC</sub>, (e) PLA<sub>PEG-b-PLLA</sub>, and (f) PLA<sub>PEG-b-PLLA+10CNC</sub>.

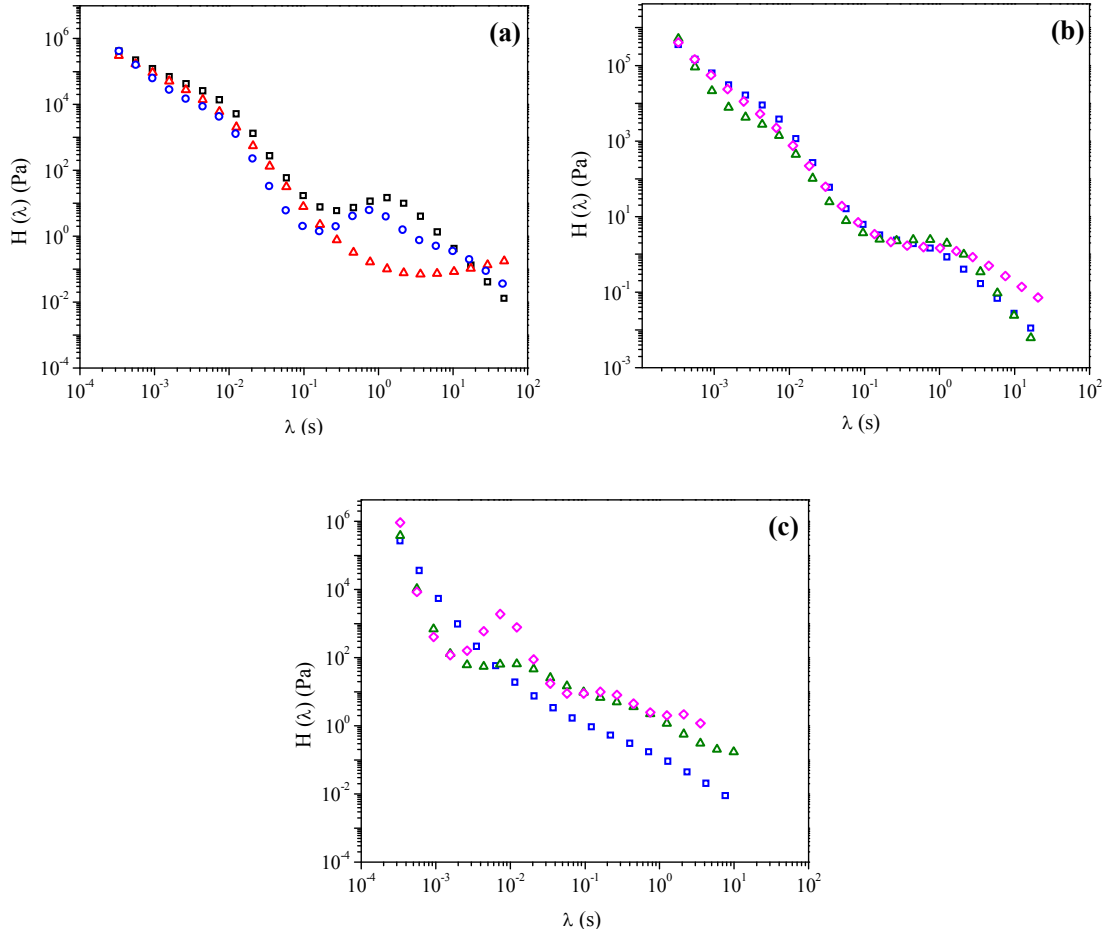


**Figure S3.** Comparative relaxation spectra for (a) PLA ( $\square$ ), PLA<sub>PEG-b-PLLA</sub> ( $\bullet$ ) and PLA<sub>Im-PLLA</sub> ( $\Delta$ ); (b) PLA<sub>PEG-b-PLLA</sub> containing 5 ( $\square$ ), 10 ( $\Delta$ ) and 20 wt% ( $\diamond$ ) CNC, and (c) PLA<sub>Im-PLLA</sub> containing 5 ( $\square$ ), 10 ( $\Delta$ ) and 20 wt% ( $\diamond$ ) CNC.

The analysis of the relaxation spectra, together with shear viscosity, provides information about polymer chain stiffness. In the case of PLA, a deeper study of these parameters can be found, such as in Dorgan *et al*<sup>2</sup> and Al-Itry *et al*.<sup>3,4</sup>

In the work of Dorgan *et al*, the relaxation of linear and branched PLA chains has been analyzed and it was concluded that increasing the number of branches leads to very different behaviors of polymer chains for longest relaxation times. Similar effects are founded here (Figure S4a), where PLA chains show longer relaxations times when compared to PLA<sub>PEG-b-PLLA</sub> and PLA<sub>Im-PLLA</sub> samples. A remark should be made for PLA<sub>Im-PLLA</sub> where the presence of much shorter chains of Im-PLLA seems to cause a meaningful effect on polymer entanglement.

Figures S4b and S4c show the effect induced by the presence of nanoparticles for both systems. No significant effect can be observed at lower relaxation times, but the presence of nanoparticles causes differentiation among the particles at longer relaxation times, where the particles-polymer chains interactions can influence the polymer chains relaxation.

For PLA<sub>PEG-b-PLLA</sub> samples (Figure 4b), the entrapment effect is observable and a higher amount of nanoparticles seems to lead to a  $H(\lambda)$  increase for a certain  $\lambda$ . However, the same effect is remarkably stronger for PLA<sub>Im-PLLA</sub> samples (Figure 4c), where a clear (and CNC content-dependent) transition region can be found around  $10^{-2}$  s. It corroborates that for this system the surfactant could trap CNC in polymers bulk, increasing their compatibility.

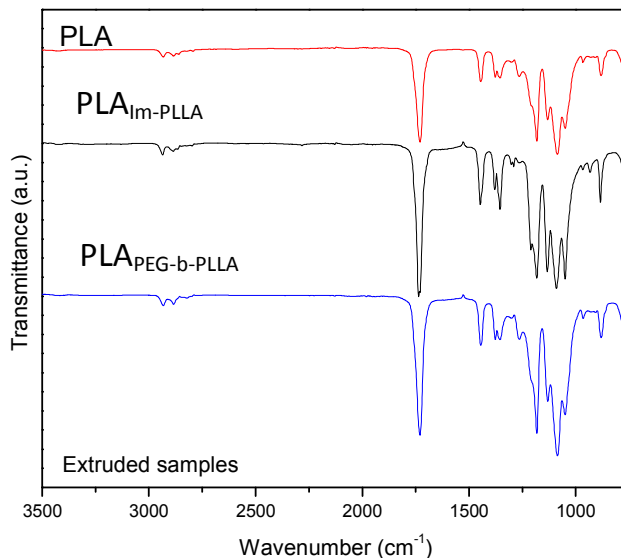


**Figure S4.** FTIR curves for PLA, PLA<sub>PEG-b-PLLA</sub> and PLA<sub>Im-PLLA</sub> after rheological tests.

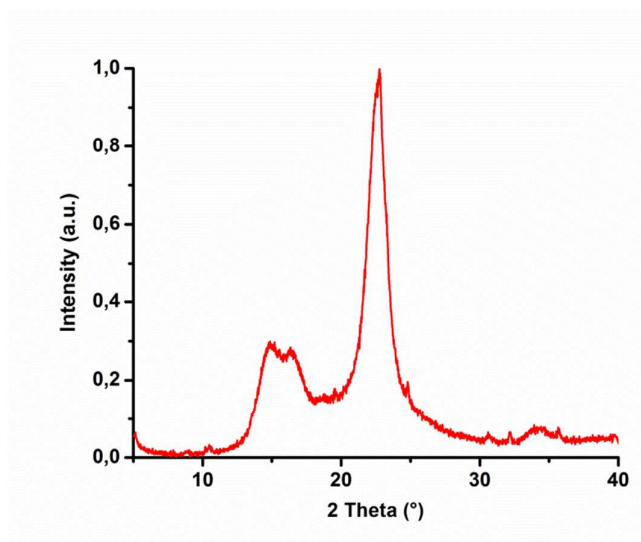


**Figure S5.** X-ray diffraction pattern for CNC extracted from ramie fibers.

## References

- (1) Dervaux, B.; Meyer, F.; Raquez, J.-M.; Olivier, A.; Du Prez, F.E.; Dubois, P. Imidazolium end-functionalized ATRP polymers as directing agents for CNT dispersion and confinement. *Macromol. Chem. Phys.* **2012**, *213*, 1259-1265.
- (2) Dorgan, J.R.; Williams, J.S.; Lewis, D.N. Melt rheology of poly(lactic acid): Entanglement and chain architecture effects. *J. rheol.* **1999**, *43*, 1141-1155.
- (3) Al-Itry, R.; Lamnawar, K.; Maazouz, A. Rheological, morphological, and interfacial properties of compatibilized PLA/PBAT blends. *Rheol. Acta* **2014**, *53*, 501-517.
- (4) Al-Itry, R.; Lamnawar, K.; Maazouz, A. Reactive extrusion of PLA, PBAT with a multi-functional epoxide: Physico-chemical and rheological properties. *Eur. Polym. J.* **2014**, *58*, 90-102.